Digital Computer Solutions of the Rigorous Equations for Scattering Problems

JACK H. RICHMOND, SENIOR MEMBER, IEEE

Abstract—**A survey of recently developed techniques for solving the rigorous equations that arise in scattering problems is presented. These methods generate a system of linear equations for the unknown current density by enforcing the boundary conditions at discrete points in the scattering body or on its surface. This approach shows promise of leading to a systematic solution for a dielectric or conducting body of arbitrary size and shape.**

The relative merits of the linear-equation solution and the variational solutions are discussed and numerical results, obtained by these two methods, are presented for straight wires of finite length.

The computation effort required with the linear-equation solution can be reduced by expanding the current distribution in a series of modes of the proper type, by making a change of variables for integration, and by employing interpolation formulas.

Solutions are readily obtained for a scattering body placed in an incident plane-wave field or in the near-zone of a source. Examples are included for both cases, using a straight wire of finite length as the scattering body.

The application of these techniques to scattering by a dielectric body is illustrated with dielectric rods of finite length.

I. Introduction

RIGOROUS SOLUTIONS exist for plane-wave scattering by the perfectly conducting plane, circular cylinder [1], elliptic cylinder [2], sphere [3], and the prolate spheroid [4]. These solutions are obtained by the method of separation of variables. The wave equation, given by

$$\nabla^2\psi + k^2\psi = 0$$

is separable only in the following eleven coordinate systems [5]: rectangular, circular cylinder, elliptic cylinder, parabolic cylinder, spherical, conical, parabolic, prolate spheroidal, oblate spheroidal, ellipsoidal, and paraboloidal. Thus, the number of scattering problems that can be solved by this classical method is severely limited. A comparable solution is not possible for the hemisphere, the circular cylinder of finite length, and other such bodies whose surfaces do not coincide with a complete constant-coordinate surface in one of the systems listed previously. In fact, difficulty is experienced in obtaining numerical data with the classical solution even for spheroids [4] and large spheres.

Variational and quasi-static solutions have shown considerable success for scatterers of various shapes, but these techniques have been limited to bodies which are small in comparison with the wavelength or are on the order of one wavelength in maximum diameter. Large scatterers are handled with the aid of physical optics, geometric optics, and the geometrical theory of diffraction. These optical solutions provide reliable data only when the scatterer has a diameter or width which is large in comparison with the wavelength. Complications arise when a portion of the surface is concave as, for example, with the hollow hemisphere. Furthermore, the solution for each new scattering shape requires a great deal of thought and ingenuity.

In the past few years, with the widespread availability of high-speed digital computers, attention has been given to a distinct approach to the scattering problem. First, a system of linear equations is obtained by enforcing the boundary conditions at many points within the scatterer or on its surface. Next, with the aid of a digital computer, this system of equations is solved to determine the current distribution on the surface or the coefficients in the mode expansion for the scattered field. Finally, one computes the distant scattering pattern.

This linear-equation technique is valid for scatterers of any convex or concave shape, and the exact solution can be approached simply by enforcing the boundary conditions at a sufficiently large number of points. The computation time is least for small scatterers (in the Rayleigh region) but it is reasonable even for bodies of resonant size or larger, depending on the capacity of the computer. Solutions can readily be obtained for perfectly conducting, imperfectly conducting, and dielectric bodies. If the body is placed in the near-zone field of a source, the solution proceeds in the same straightforward manner as in the plane-wave case.

Thus, the linear-equation solution shows promise for accurate, systematic calculations for bodies of arbitrary material, size, and shape. This paper reviews briefly the recent progress in this technique, discusses several methods for reducing the computation effort, and illustrates the techniques by considering a wave to be incident on a straight wire or a dielectric rod of finite length.

II. Survey of Recent Progress

Some of the recent applications of the linear-equation technique follow:

Mei and Van Bladel [6] calculated the surface-current density and the scattering patterns of perfectly conducting rectangular cylinders of infinite length. Re-

Manuscript received March 4, 1965; revised April 30, 1965.
The author is with the Antenna Lab., Dept. of Electrical Engineering, The Ohio State University, Columbus, Ohio.

sults were obtained for incident plane waves having parallel and perpendicular polarization with respect to the cylinder axis.

Andreasen [7] solved for the surface currents and the scattered fields of perfectly conducting cylinders of elliptic and parabolic cross sections, and arrays of parallel cylinders. A plane wave was assumed to be normally incident on these cylinders of infinite length, and results were published for parallel and perpendicular polarization. Cylinders with a circumference up to about 40 wavelengths could be handled with the aid of a CDC 1604 computer.

Richmond [8] obtained solutions for arrays of thin parallel wires of infinite length and for conducting cylinders of semicircular and I-beam cross section. The incident plane wave was assumed to propagate at any angle θ with respect to the cylinder axis, with the incident magnetic field intensity perpendicular to the cylinder axis.

Richmond [9] calculated the field distribution induced in a dielectric cylinder of infinite length, and the distant scattering patterns. The incident plane wave was assumed to be polarized parallel with the cylinder axis. Results were published for dielectric cylindrical shells of circular and semicircular cross section and for plane dielectric slabs of infinite height and finite thickness and width. Both lossless and low-loss dielectric cylindrical shells were considered, and results are given for homogeneous and inhomogeneous cases. In one case, the incident field is that of a parallel line source near the dielectric cylinder.

Mullin, Sandburg, and Velline [10] calculated the bistatic echo width of conducting elliptic cylinders for incident plane waves having parallel and perpendicular polarization. The scattered field external to the cylinder was expanded in a series of outward-traveling modes. In its present form, this technique gives accurate results only for cylinders which do not depart greatly from the circular cross-section shape.

Kennaugh [11] made one of the earliest studies of digital-computer solutions of scattering problems in which the boundary conditions are enforced at discrete points. Successful calculations were carried out for prolate and oblate spheroids illuminated by a plane wave incident along the symmetry axis. A system of 21 linear equations was obtained by setting the tangential electric field intensity equal to zero at evenly spaced points on the surface. Eight coefficients were determined for the scattered field expansion in spherical modes by obtaining a least-squares solution for the 21 equations.

Andreasen [12] has set up a computer program for calculating the current distribution and the scattered field of a perfectly conducting body of revolution. The incident plane wave may have arbitrary polarization and angle of incidence. The current distribution is expressed as a series of mode currents. The maximum perimeter of the conducting body is approximately 20 wavelengths.

Waterman [13] has also developed a program for solving for the current distribution and the scattered field of a perfectly conducting figure of revolution. The scattered field is expressed as an integral of the surface current density. The electric field intensity is forced to vanish throughout a portion of the interior of the conducting body to obtain a system of linear equations. Green's identity is employed to decouple the pair of integral equations, to reduce the number of unknown currents by a factor of 2, and, after calculating them for one polarization, to obtain by inspection the current expansion coefficients for the orthogonal polarization.

Schultz, Ruckgaber, Richter, and Schlindler [14] have employed the linear-equation technique to obtain the scattering patterns of conducting cones with spherical caps. The field was expanded in spherical mode functions of the proper type for each of the two regions of space. Relations were obtained for the field expansion coefficients by applying the appropriate boundary conditions. The infinite series for the field was approximated with the finite series of spherical modes, and the system of linear equations for the coefficients was solved with the aid of an IBM 7090 computer.

Baghdasarian and Angelakos [15] have obtained solutions for the current induced on a circular conducting loop by an incident plane wave, and for the scattered field of the loop. Excellent results were obtained for normal and oblique incidence.

Two distinct approaches have been employed to obtain a system of linear equations for these scattering problems. One may expand the scattered field in a series of mode functions (cylindrical modes, spherical modes, etc.) and obtain a system of linear equations for the coefficients in this series. Alternatively, the surface current density can be expanded in a series of mode functions and a system of linear equations is then obtained for the coefficients in this series. In the latter case, the scattered field is expressed as an integral over the surface current density and one is led to an integral equation. The integral expression for the scattered field is valid at every point in space, whereas a mode expansion for the scattered field is usually valid only in a particular region. Mode-series expansions for the scattered field have been employed by Sommerfeld [16], Mullin [10], Kennaugh [11], Schultz [14], and others. Integral expressions for the scattered field were used by Mei and Van Bladel [6], Andreasen [7], [12], Richmond [8], [9], Waterman [13], and Baghdasarian and Angelakos [15].

III. An Example: the Slender Straight Wire of Finite Length

Consider a harmonic electromagnetic wave in free space incident on a slender, finite, perfectly conducting wire as illustrated in Fig. 1. The time dependence $e^{j\omega t}$

is understood. The wire radius a is assumed to be much smaller than the length L and the wavelength λ. The wire is considered to be a hollow metal tube, open at both ends. The scattered field may be generated by the surface current J on the circular cylinder $\rho=a$, radiating in free space. With good accuracy, the surface current density on the thin wire can be considered to have only an axial component. Furthermore, the current density (representing the sum of the currents on the inner and outer surfaces of the thin-wall metal tube) can be assumed to be distributed uniformly around the circumference of the wire. That is,

$$J = \hat{z}J(z) \tag{1}$$

where $\hat{z}$ represents a unit vector parallel to the wire axis. Solutions can also be obtained for solid or hollow wires of large radii, but the purpose here is to illustrate the techniques by considering a relatively simple example.

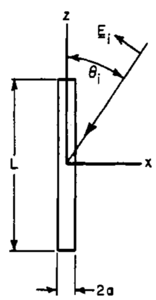

Fig. 1. A plane wave has oblique incidence on a conducting wire of length L and radius a.

The z component of the field scattered by the wire is given by the following expression:

$$E_z^s(\rho, z) = \frac{a\lambda\sqrt{\mu/\epsilon}}{8\pi^2 j}\int_0^{2\pi}\int_{-L/2}^{L/2} J(z')F(r, z, z')\, dz' d\phi' \tag{2}$$

where ρ and z are the cylindrical coordinates of the observation point, (a, ϕ', z') are the cylindrical coordinates of the source point, r is the distance between these two points:

$$r = \sqrt{\rho^2 + a^2 - 2a\rho\cos\phi' + (z'-z)^2} \tag{3}$$

$$F(r, z, z') = \left[2r^2(1 + jkr) - (3 + 3jkr - k^2r^2)(r^2 - (z'-z)^2)\right]\frac{e^{-jkr}}{r^5} \tag{4}$$

and $k=2\pi/\lambda$. The angular coordinate ϕ of the observation point has been taken equal to zero in (3), since the scattered field is independent of ϕ under the assumed conditions. Equation (2) can be derived with the aid of the vector potential or by starting with the expression for the field of an infinitesimal electric dipole and employing the superposition theorem.

The current density is related to the current $I(z)$ by

$$J(z) = \frac{I(z)}{2\pi a}\,. \tag{5}$$

If the observation point is on the axis of the wire, $\rho=0$, and the preceding expression for the scattered field reduces to

$$\begin{aligned} E_z^s(0, z) &= \frac{\lambda\sqrt{\mu/\epsilon}}{8\pi^2 j}\int_{-L/2}^{L/2} I(z')\frac{e^{-jkr}}{r^5} \cdot\left[(1 + jkr)(2r^2 - 3a^2) + k^2a^2r^2\right] dz' \\ &= -E_z^i(0, z) \end{aligned} \tag{6}$$

where

$$r = \sqrt{a^2 + (z'-z)^2}. \tag{7}$$

The interior region of the hollow wire ($\rho<a$) can be regarded as a circular waveguide, and the field there can be expanded in a series of waveguide modes beyond cutoff. In this way, it can be shown that the total field essentially vanishes in the interior region if the distance from the nearest end of the wire exceeds 3 or 4 radii.

The electric field intensity is the sum of the incident and scattered intensities:

$$\boldsymbol{E} = \boldsymbol{E}^i + \boldsymbol{E}^s. \tag{8}$$

Thus,

$$\boldsymbol{E}^s(\rho, z) = -\boldsymbol{E}^i(\rho, z) \tag{9}$$

for $\rho<a$ and for $|z|<0.5L-4a$. It follows from (9) that we may set the right-hand side of (6) equal to $-E_z^i(0, z)$.

It will be noted that we are proposing to force the axial electric field intensity to vanish only on the axis of the wire, although in actuality the vector $\boldsymbol{E}$ must vanish everywhere in the interior region except in the vicinity of the open ends. If the wire is slender, it can be shown that the field will almost vanish everywhere within the wire if its axial component is forced to vanish on the axis. Furthermore, the computations are simplified when this condition is enforced on the axis, since the single integral in (6) is easier to evaluate than the double integral in (2).

Even if the current distribution $I(z)$ were known, the integral in (6) could not be evaluated analytically, except in the form of an infinite series. However, numerical integration is possible and feasible with the aid of a digital computer.

In many problems, the incident field intensity $E_z^i(0, z)$ in (6) is known. It may, for example, represent the field of an incident plane wave having oblique incidence as in Fig. 1. The current distribution $I(z)$ induced on the wire is then an unknown function which is to be determined. Techniques for solving this integral equation to any desired degree of accuracy, with the assistance of a digital computer, are considered next.

IV. Change of Variables

Integration is often facilitated by making a change of variables. This is helpful both in numerical integration and in analytic integration. Although the optimum change of variable may be difficult to determine, one that has been found very helpful in the problem of the slender finite wire is the following:

$$z' - z = a \tan \theta' \tag{10}$$

$$dz' = a \sec^2 \theta' \, d\theta'. \tag{11}$$

With this change of variables, the integral equation (6) for the slender wire becomes:

$$\frac{\lambda\sqrt{\mu/\epsilon}}{8j\pi^2 a^2} \int I(z') e^{-jka/\cos\theta'} \cdot [(jka + \cos\theta')(2 - 3\cos^2\theta') + k^2a^2\cos\theta'] \, d\theta' = - E_z{}^i(0, z). \tag{12}$$

The limits of integration are

$$\theta_1' = - \tan^{-1} \frac{0.5L + z}{a} \tag{13}$$

$$\theta_2' = \tan^{-1} \frac{0.5L - z}{a} \cdot \tag{14}$$

If the integral is evaluated numerically with the Newton-Cotes formulas [17], the integrand is sampled at equally spaced points of the variable of integration. The integrand varies most rapidly when the source point is in the vicinity of the observation point. The number of terms required in numerical integration is fixed by the requirement that the integrand be adequately sampled in the region where it varies most rapidly. If the integration is on z' as in (6), a large number of terms are required to obtain adequate sampling. If one makes the change of variables described previously, equal intervals are taken in θ' (instead of in z'), providing a dense sampling in the vicinity of $z' = z$ where the integrand varies most rapidly, and tapering to a lighter sampling as one moves away from this region. Thus, fewer terms are required in the numerical integration.

V. Mode Expansion of the Current Distribution

The current on a hollow wire with thin walls must vanish at the ends. A suitable expansion for the current is the Fourier series given by

$$I(z) = \sum_{n=1}^{N} \left[I_n \cos (2n - 1) \frac{\pi z}{L} + I_n' \sin \frac{2n\pi z}{L} \right]. \tag{15}$$

Inserting this expression in (12) we obtain:

$$\frac{\lambda\sqrt{\mu/\epsilon}}{8i\pi^2 a^2} \sum_{n=1}^{N} \left[I_n \int G(\theta') \cos (2n - 1) \frac{\pi z'}{L} \, d\theta' + I_n' \int G(\theta') \sin \frac{2n\pi z'}{L} \, d\theta' \right] = - E_z{}^i(0, z) \tag{16}$$

where

$$G(\theta') = e^{-jka/\cos\theta'} \cdot [(\cos\theta' + jka)(2 - 3\cos^2\theta') + k^2a^2\cos\theta']. \tag{17}$$

The limits of integration are again given by (13) and (14).

If (16) is enforced at N points $z = z_1, z_2, \cdots, z_N$ along the wire axis, a system of N linear equations is obtained which have the following form:

$$\sum_{n=1}^{N} (C_{mn} I_n + C_{mn}' I_n') = - E_z{}^i(0, z_m). \tag{18}$$

C_{mn} represents the scattered field at a point $(0, z_m)$ generated by the current distribution $I = \cos (2n - 1)\pi z/L$, and C_{mn}' is the scattered field at z_m generated by the current $I = \sin 2n\pi z/L$. The complex mode amplitudes I_n and I_n' are obtained by solving this system of linear equations. The method of Crout [18] has been found to be convenient and efficient for solving the system of linear equations on a digital computer.

The Fourier series for the current $I(z)$ converges rapidly at first, and then more slowly, as shown in Table I. In calculating the data shown in Table I, the integrals in (16) were evaluated with the fifth-order Newton-Cotes formula (which is exact for integrals of fifth-degree polynomials) using 1000 terms for the integration along the wire.

TABLE I

Fourier Coefficients for the Current $I(z)$ for an Incident Plane Wave: $L = 0.5\lambda$; $a = 0.005\lambda$.

	$\theta_i = 30°$				$\theta_i = 90°$	
Mode Number n	I_n/λ (mA)	Phase I_n (degrees)	I_n'/λ (mA)	Phase I_n' (degrees)	I_n/λ (mA)	Phase I_n (degrees)
1	1.4272	−35.3	0.1408	179.1	3.4762	−36.1
2	0.0800	135.8	0.0230	−0.9	0.1700	146.9
3	0.0373	−41.1	0.0104	179.1	0.0849	−34.2
4	0.0235	140.0	0.0064	−0.9	0.0547	145.4
5	0.0169	−39.3	0.0045	179.1	0.0399	−34.8
6	0.0132	141.0	0.0035	−0.9	0.0312	145.1
7	0.0108	−38.8	0.0029	179.1	0.0256	−35.0
8	0.0092	141.3	0.0024	−0.9	0.0218	145.0
9	0.0080	−38.6	0.0021	179.1	0.0190	−35.1
10	0.0072	141.5	0.0019	−0.9	0.0169	144.9
11	0.0065	−38.4	0.0017	179.1	0.0152	−35.1
12	0.0060	141.6	0.0016	−0.9	0.0140	144.9
13	0.0056	−38.3	0.0015	179.1	0.0130	−35.1
14	0.0053	141.7	0.0014	−0.9	0.0121	144.9
15	0.0050	−38.3	0.0007	179.1	0.0115	−35.1

In order to reduce the number of linear equations which must be solved, it would be advantageous to expand the current $I(z)$ in a series of functions which converges more rapidly than the Fourier series given in Table I. Table II lists the coefficients for the current expansion in several types of series. The Chebyshev and Legendre series appear most promising, but this matter requires further investigation.

TABLE II

COEFFICIENTS FOR THE CURRENT $I(z)$ FOR AN INCIDENT PLANE WAVE: $L=0.5\lambda$; $a=0.005\lambda$; $\theta_i=90°$

Mode No. n	Fourier	Maclaurin	Chebyshev	Hermite	Legendre
1	3.476	3.374	1.7589	8.2929	2.2762
2	0.170	4.037	1.5581	14.3644	2.1005
3	0.085	3.128	0.0319	4.4135	0.0655
4	0.055	4.101	0.0112	0.3453	0.0421
5	0.040	1.871	0.0146	0.0073	0.0372

Table II gives the magnitude of I_n in mA for the following series:

Fourier:
$I(z) = I_1 \cos \pi x/2 + I_2 \cos 3\pi x/2 + I_3 \cos 5\pi x/2 + +$
Maclaurin:
$I(z) = I_1 + I_2x^2 + I_3x^4 + +$
Chebyshev:
$I(z) = I_1T_0(x) + I_2T_2(x) + I_3T_4(x) + +$
Hermite:
$I(z) = I_1H_0(x) + I_2H_2(x) + I_3H_4(x) + +$
Legendre:
$I(z) = I_1P_0(x) + I_2P_2(x) + I_3P_4(x) + +$
where
$x = 2z/L.$

VI. THE DISTANT SCATTERED FIELD

The distant scattered field of a slender wire of finite length has only a θ component which is given by

$$E^s(\theta_s) = \frac{j\omega\mu}{4\pi r_0} e^{-jkr_0} \sin \theta_s \int_{-L/2}^{L/2} I(z') e^{jkz' \cos \theta_s} dz' \quad (19)$$

where r_0 is the distance from the origin (at the center of the wire) and θ_s is the scattering angle measured from the axis of the wire.

If the current $I(z)$ is represented by a piecewise uniform function,[1] the distant scattered field is given by

$$E^s(\theta_s) = \frac{j\omega\mu L}{4\pi r_0 N} e^{-jkr_0} \sin \theta_s \sum_{n=1}^{N} I_n e^{jkz_n \cos \theta_s} \quad (20)$$

where I_n is the current on segment n, z_n is the coordinate of the center of segment n, and N is the total number of segments.

If the current distribution is expressed as a Fourier series as in (15), the distant scattered field is given by

$$E^s(\theta_s) = \frac{-jL\sqrt{\mu/\epsilon}}{\pi r_0} e^{-jkr_0} \sin \theta_s \cdot \sum_{n=1}^{N} (-1)^n \left[\frac{(2n-1)I_n \cos(\pi L' \cos \theta_s)}{(2n-1)^2 - (2L' \cos \theta_s)^2} + \frac{2jnI_n' \sin(\pi L' \cos \theta_s)}{4n^2 - (2L' \cos \theta_s)^2} \right] \quad (21)$$

where $L' = L/\lambda$.

If the incident field is that of a plane wave of amplitude E_0, the echo area of the wire is given by

$$\sigma(\theta_s) = \lim_{r_0 \to \infty} 4\pi r_0^2 = \frac{|E^s(\theta_s)|^2}{|E_0|^2}. \quad (22)$$

[1] See Baghdasarian and Angelakos [15] for an example employing a piecewise uniform function for the current.

Figure 2 shows several calculated scattering patterns based on the Fourier series expansion for the current. The results shown in this figure correspond to the current distribution listed in Table I. Fifteen cosine modes and 15 sine modes were used, and 1000 terms were employed in each integration along the wire.

A comparison of the measured and calculated backscatter echo area of straight wires is illustrated in Fig. 3. The measured data are those published by Kouyoumjian [19]. In the calculations, 15 cosine terms were used in the Fourier series for the current and 1000 terms were employed in the numerical integrations. The variational solution of Tai [20] is also shown. It may be noted that the linear-equation solution shows better agreement with the experimental measurements.

In principle, a high degree of accuracy may be obtained with the variational solution by including a sufficient number of terms in the trial function for the current distribution. In practice, however, the computational effort increases rapidly as the number of terms is increased. In the scattering problem for the slender wire, only two terms are usually included in the trial function for normal incidence and four terms for oblique incidence. On the other hand, it is practical to include a much greater number of terms in the current expansion with the linear-equation technique.

An interesting property of the zero-order variational solution [20] is that it yields for normal incidence an echo area which is independent of the wire radius when the wire length is 0.5 λ, 1.5 λ, etc. Experimental measurements [21], however, show that the echo area is definitely a function of the radius even when the length is an odd number of half wavelengths. Higher-order variational calculations by Hu [22] show quite accurately the dependence on the radius for wire lengths up to two wavelengths. The linear-equation solution also shows a dependence on the radius which agrees with experimental data and the calculations of Hu. This dependence is slight for the half-wave wire, but not for the 3/2 wavelength case.

Van Vleck, Bloch, and Hamermesh [23], King [24], and Dike and King [25] have obtained an approximate solution for the thin wire by solving the integral equation to obtain the leading terms in the series for the current distribution. Although Lindroth [26] has obtained useful results by this method for wire lengths up to 2.5 wavelengths, it does not appear to show much promise for longer wires. The rigorous solution of Hallén [27] has apparently not yet been exploited to obtain accurate solutions for scattering by long wires.

Solutions were readily obtained with the linear-equation technique for wires of length $L=2.865\ \lambda$ ($kL=18$) and radii $a=0.00415\ \lambda$ and $0.0105\ \lambda$ ($ka=0.026$ and 0.066). For normal incidence, the backscatter echo areas were found to be 1.65 and 2.63 square wavelengths, respectively, showing excellent agreement with the measurements by Ås and Schmitt [21]. For a length

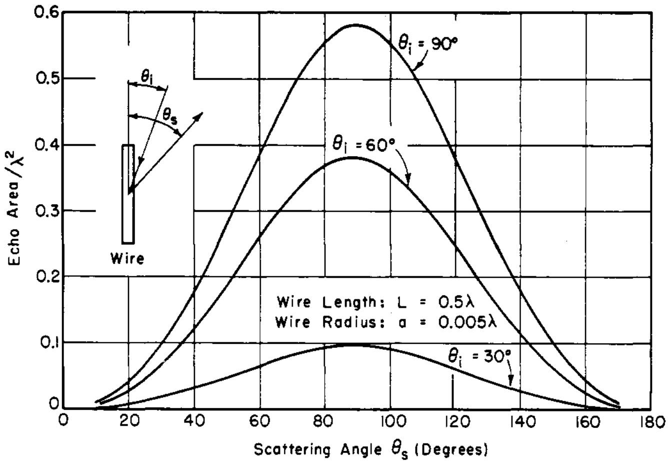

Fig. 2. Calculated bistatic echo area of straight wire vs. scattering angle for incident plane wave with angle of incidence of 30°, 60°, and 90°.

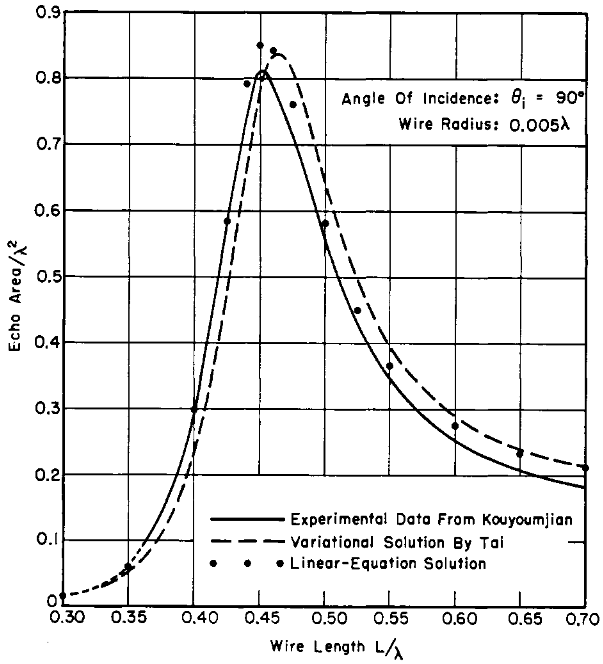

Fig. 3. Measured and calculated backscatter echo area of straight wire for normal incidence.

$L = 3.82\ \lambda$ ($kL = 24$) and radius $a = 0.0035\ \lambda$ the calculated result is 2.8 square wavelengths and the measured result by Sevick [21] is 2.01 square wavelengths. The difference is believed to arise from phase errors along the wire in the experimental measurements.

VII. The Reciprocity Theorem

When a plane wave is incident on a straight wire, the distant scattered field is a function of the angle of incidence ϕ_i and the angle of scattering θ_s. The reciprocity theorem assures us that the phase and strength of the scattered field is unchanged when the angle of incidence and the angle of scattering are interchanged. Thus,

$$E_s(\theta_i, \theta_s) = E_s(\theta_s, \theta_i). \tag{23}$$

This provides a useful check on the accuracy of numerical scattering calculations, except in cases where the reciprocity theorem has been incorporated into the solution. Furthermore, the reciprocity theorem can be utilized to speed up the calculations. Of course, the reciprocity theorem is automatically satisfied by any rigorous solution.

In the linear-equation technique, the currents on the wire satisfy a system of equations of the following type:

$$\sum_{n=1}^{N} C_{mn} I_n = -E_z^i(\theta_i, z_m) \tag{24}$$

where $E_z^i(\theta_i, z_m)$ represents the tangential electric field intensity of the incident plane wave. The I_n may represent the mode-current amplitudes or the piecewise uniform currents induced on the wire. From (24) it is obvious that the currents will be a function of the angle of incidence θ_i. The distant scattered field in any angular direction θ_s is given by (19)–(21), which can be written in the following general form:

$$E^s(\theta_i, \theta_s) = \sum_{n=1}^{N} I_n(\theta_i) S_n(\theta_s). \tag{25}$$

The scattering functions $S_n(\theta_s)$ are given by (20) and (21) when the piecewise uniform or the Fourier series representation is employed for the current.

From (23) and (25), it is required that

$$\sum_{n=1}^{N} I_n(\theta_i) S_n(\theta_s) = \sum_{n=1}^{N} I_n(\theta_s) S_n(\theta_i). \tag{26}$$

It does not necessarily follow that $I_n(\theta_i) = A_n S_n(\theta_i)$, although this is the most obvious solution of (26). It is possible to determine by means of (26) the currents I_n for all angles of incidence once they have been calculated for one angle of incidence. However, this approach will not be pursued here since the technique described in Section VIII accomplishes the same end result with equal efficiency.

It is not difficult to show that the reciprocity theorem and (26) are satisfied precisely by the solution using the piecewise uniform representation, even when the solution is inaccurate as a result of dividing the wire into a small number of segments. Thus the reciprocity theorem does not in this case provide a useful check on the accuracy. On the other hand, the reciprocity theorem is not precisely satisfied by the solution in Section V, which employs a Fourier series expansion for the current. For the case illustrated in Table I and Fig. 2, the reciprocity theorem is satisfied to a high degree of accuracy, but it is not satisfied so accurately when the same problem is solved with an inadequate number of terms in the Fourier series and in the numerical integration. This is illustrated in Table III.

TABLE III
ECHO AREA OF STRAIGHT WIRE WITH PLANE-WAVE INCIDENT
$L = 0.5\lambda \quad a = 0.005\lambda$

Number of Terms in Integration	Number of Terms in Fourier Series	θ_i	θ_s	Calculated Echo Area/λ^2
300	4 cos and 4 sin	30°	60°	0.07390
300	4 cos and 4 sin	60	30	0.07428
1000	15 cos and 15 sin	30	60	0.06763
1000	15 cos and 15 sin	60	30	0.06762

VIII. Repeated Solutions for Different Angles of Incidence

Most of the computation effort in the linear-equation technique is concerned with the integrations over the surface of the conducting body and the solution of the system of linear equations. Once a solution has been obtained for the currents on a given wire with a given incident field, very little additional effort is required to obtain the solution for a new incident field or a new angle of incidence. The integrations need not be repeated, since they depend only on the wire length and radius and the frequency of the incident wave. The matrix inversion for the linear equations need not be repeated, since the coefficients depend only on these same factors. Thus, it would be inefficient to repeat the entire calculation for each new angle of incidence.

This can be illustrated with a simple example. Consider the solution of the following system of linear equations:

$$C_{11}I_1 + C_{12}I_2 = E_1 \tag{27}$$

$$C_{21}I_1 + C_{22}I_2 = E_2. \tag{28}$$

In solving such a system by the method of Crout [18], one first calculates an "auxiliary" matrix C' whose elements are defined as follows:

$$C_{11}' = C_{11} \tag{29}$$

$$C_{12}' = C_{12}/C_{11} \tag{30}$$

$$C_{21}' = C_{21} \tag{31}$$

$$C_{22}' = C_{22} - C_{21}'C_{12}'. \tag{32}$$

The preceding calculations for the auxiliary matrix need be carried out only once, since the elements of the matrices C and C' depend only on the scattering structure. The elements E_1 and E_2 in (27) and (28) represent the incident field intensity at certain points along the axis of the wire. For each new incident field (or each new angle of incidence in the plane-wave case), one first calculates

$$E_1' = E_1/C_{11}' \tag{33}$$

$$E_2' = (E_2 - C_{21}'E_1')/C_{22}'. \tag{34}$$

The solution for the system of linear equations is then given by

$$I_2 = E_2' \tag{35}$$

$$I_1 = E_1' - E_2'C_{12}'. \tag{36}$$

When a large system of linear equations is involved, the efficiency is greatly increased by repeating only the calculations like those in (33) through (36) for each new incident field or angle of incidence, instead of treating each one like an entirely new problem.

This method of Crout is easily programmed for a digital computer. Even for large systems of linear equations, it has been found to be efficient with respect to computation time and memory storage requirements. (As each element in the auxiliary matrix is calculated, it is stored in the location previously occupied by the corresponding element of the original matrix.)

The incident field $E_z^i(0, z)$ enters into the problem only in the right-hand side of the linear equations. Thus, it is straightforward to solve for the currents induced on a wire by any type of incident wave. Section IX describes the results obtained when the incident field is generated by a short dipole parallel with a slender wire, as a function of the distance between the wire and the dipole.

IX. Scattering by Wire in Near-Zone Field

Figure 4 shows the current distribution induced on a wire when the source of the incident field is an electric dipole parallel with the wire. If the dipole is at a distance d from the wire, as shown in Fig. 4, the tangential component of the incident field is given by

$$E_z^i(0, z) = \frac{Ke^{-jkr}}{r^5}[(1 + jkr)(2z^2 - d^2) + k^2r^2d^2] \tag{37}$$

where

$$r = \sqrt{z^2 + d^2}. \tag{38}$$

For the solutions shown in Fig. 4, the dipole strength was adjusted to maintain the incident field E_z^i at unit strength at the center of the wire as the distance d was varied. It may be noted in Fig. 4 that the current distribution approaches that for an incident plane wave as the distance to the dipole increases. It is interesting that the current distribution in the plane-wave case differs noticeably from the cosine current generally assumed for the half-wave wire in the variational solution.

It is believed that considerable effort would be required to set up a variational solution for the straight wire near a dipole source. In particular, a trial function would have to be found for the current distribution which would permit a reasonably accurate representation of the true current function and at the same time would contain not more than about four unknown constants. On the other hand, a minimum of effort is required with the linear-equation formulation for each new type of incident field considered.

X. Scattering by a Finite Dielectric Rod

The linear-equation technique applies equally well in calculating the scattered fields of a dielectric body. If the permeability of the body is the same as that of free space, the scattered field may be generated by an equiv-

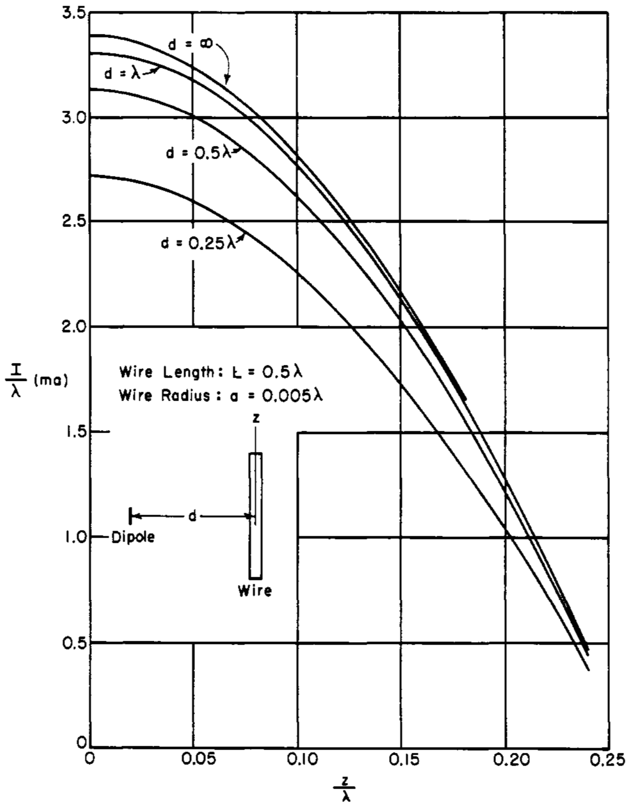

Fig. 4. Current distribution induced on straight wire by parallel electric dipole.

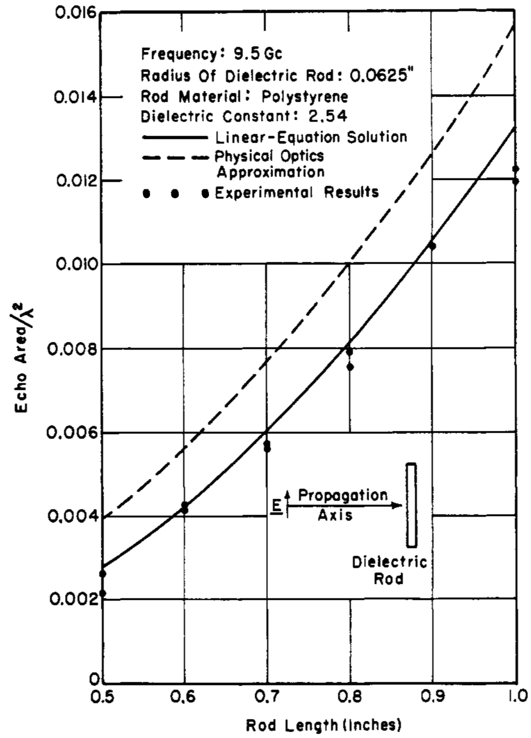

Fig. 5. Calculated and measured echo area of dielectric rod as a function of length.

alent electric current density J radiating in free space, where

$$J = j\omega(\epsilon - \epsilon_0)\boldsymbol{E}. \tag{39}$$

$\boldsymbol{E}$ represents the total electric field intensity in the dielectric body, given by the sum of the incident and scattered field intensities as follows:

$$\boldsymbol{E} = \boldsymbol{E}^i + \boldsymbol{E}^s. \tag{40}$$

The techniques may be illustrated by considering the problem of scattering by a dielectric rod of finite length. From a study of the rigorous solution for a plane-wave incident on a dielectric rod of infinite length, it may be deduced that the fields in a slender rod are nearly independent of the angle ϕ. On the axis of the rod the tangential scattered field is given, with the aid of (39) by

$$\begin{aligned} E_z{}^s(0, z) &= 0.5(\epsilon_r - 1)\int_{-L/2}^{L/2}\int_0^a E_z(\rho, z')F(r, \rho)\,d\rho dz' \\ &= E_z(0, z) - E_z{}^i(0, z) \end{aligned} \tag{41}$$

where a denotes the radius of the rod, L is the length, ϵ_r is the relative permittivity,

$$F(r, \rho) = \rho[(1 + jkr)(2r^2 - 3\rho^2) + k^2\rho^2r^2]\,\frac{e^{-jkr}}{r^5} \tag{42}$$

and

$$r = \sqrt{\rho^2 + (z' - z)^2}. \tag{43}$$

Let it be assumed that a plane wave is normally incident on the dielectric rod with the incident electric field vector parallel with the axis of the rod. In this case, the total field $E_z(\rho, z)$ must be an even function of z. With the aid of Maxwell's equations, it can be shown that the total field in the rod can be expanded in a mode series as follows:

$$E_z(\rho, z) = \sum_0^{N-1} E_n \cos\frac{2n\pi z}{L}\, J_0[k\rho\sqrt{\epsilon_r - (n/L')^2}] \tag{44}$$

where $J_0(x)$ represents the Bessel function of zero order and $L' = L/\lambda$. In a rigorous solution, an infinite number of modes would be employed in (44), but here we shall include only a finite number N. The summation in (44) is substituted for $E_z(0, z)$ and $E_z(\rho, z')$ in (41).

The integral equation (41) is enforced at N points $z = z_m$ on the axis of the rod (between $z = 0$ and $z = L/2$) to obtain N linear equations for the mode amplitudes E_n. The integrals in (41) may be evaluated numerically with the Newton-Cotes formulas, but it must be recognized that a singularity occurs at $z' = z$ and $\rho = 0$ where r goes through zero. The difficulties involved in handling this integrable singularity may be avoided by changing the limits of integration to $\delta < \rho < a$ where δ is much smaller than the radius a. The solution then will correspond to that for a dielectric rod having a tiny hole of radius δ drilled along its axis. If δ is much smaller than a, the volume of dielectric material thus removed is small compared with the total volume and the error from this source should be negligible. The change of variables $dz' = \rho \sec^2\theta' d\theta'$ is found to be helpful.

Figure 5 shows the echo area calculated in this manner for polystyrene rods of $\frac{1}{8}$-inch diameter at a frequency of 9.5 Gc. It may be noted that the calculations show excellent agreement with the experimental measurements which are also presented in Fig. 5. The double integration (on ρ and θ') in (41) was performed with the fifth-order Newton-Cotes formula.

Comparatively poor results are obtained from the physical-optics solution for this problem, shown by the dashed curve in Fig. 5. In the physical-optics solution, the field in the rod is taken to be the same as that in a rod of infinite length. The scattered field is then considered to be the field generated by the equivalent current (39) radiating in free space. This current is assumed to exist only in the region occupied by the finite dielectric rod. Evidently, the field in the finite rod differs significantly from that in the infinite rod.

XI. Conclusions

In recent years, we have begun to exploit the high-speed digital computer to obtain accurate solutions for the fields scattered by bodies of complex shapes. Approaches are now feasible which overcome the limitations inherent in the method of separation of variables, the variational solutions, physical optics, geometrical optics, and the geometrical theory of diffraction.

In the method considered here, a system of linear equations is obtained by enforcing the boundary conditions at a finite number of points on the surface or in the interior of the scattering body. The solution of this set of equations yields the current distribution induced on the conducting surface.

This paper surveys the recent progress in this area and discusses several techniques for increasing the efficiency of the calculations and extending the maximum dimensions of the scattering bodies that can be handled. Among these techniques are the change of variables for integration, expansion of the current in a series of modes, and interpolation.

These techniques are illustrated by considering a comparatively simple example: the slender wire of finite length. Numerical results are shown for the current distribution induced on such wires and for the backscatter and bistatic echo area. Calculations are illustrated for a half-wave wire near an electric dipole which acts as the source of the field.

This linear-equation technique is also applicable to dielectric bodies. This is illustrated by considering a plane-wave incident on a dielectric rod of finite length. The results show excellent agreement with experimental measurements.

Acknowledgment

The author wishes to express his sincere appreciation for the extensive digital computations provided by The Ohio State University Computer Center in support of this investigation. The experimental measurements of backscatter from finite dielectric rods were carried out by S. A. Redick of The Ohio State University Antenna Laboratory, whose assistance is gratefully acknowledged.

References

[1] R. F. Harrington, *Time-Harmonic Electromagnetic Fields.* New York: McGraw-Hill, 1961, pp. 232–236.
[2] G. Sinclair, "The patterns of antennas located near cylinders of elliptical cross section," *Proc. IRE*, vol. 39, pp. 660–668, June 1951.
[3] J. A. Stratton, *Electromagnetic Theory.* New York: McGraw-Hill, 1941, pp. 563–572.
[4] K. M. Siegel, F. V. Schultz, B. H. Gere, and F. B. Sleator, "The theoretical and numerical determination of the radar cross section of a prolate spheroid," *IRE Trans. on Antennas and Propagation*, vol. AP-4, pp. 266–275, July 1956.
[5] P. M. Morse and H. Feshbach, *Methods of Theoretical Physics.* New York: McGraw-Hill, 1953, pt. I, pp. 655–664.
[6] K. K. Mei and J. G. Van Bladel, "Scattering by perfectly-conducting rectangular cylinders," *IEEE Trans. on Antennas and Propagation*, vol. AP-11, pp. 185–192, March 1963.
[7] M. G. Andreasen, "Scattering from parallel metallic cylinders with arbitrary cross sections," *IEEE Trans. on Antennas and Propagation*, vol. AP-12, pp. 746–754, November 1964.
[8] J. H. Richmond, "Scattering by an arbitrary array of parallel wires," *IEEE Trans. on Microwave Theory and Techniques*, vol. MTT-13, pp. 408–412, July 1965.
[9] ——, "Scattering by a dielectric cylinder of arbitrary cross section shape," *IEEE Trans. on Antennas and Propagation*, vol. AP-13, pp. 334–341, May 1965.
[10] C. R. Mullin, R. Sandburg, and C. O. Velline, "A numerical technique for the determination of scattering cross sections of infinite cylinders of arbitrary geometrical cross section," *IEEE Trans. on Antennas and Propagation*, vol. AP-13, pp. 141–149, January 1965.
[11] E. M. Kennaugh, "Multipole field expansions and their use in approximate solutions of electromagnetic scattering problems," Ph.D. dissertation, Dept. of Elec. Engrg., The Ohio State University, Columbus, December 1959.
[12] M. G. Andreasen, "Scattering from bodies of revolution by an exact method," *IEEE Trans. on Antennas and Propagation*, vol. AP-13, pp. 303–310, March 1965.
[13] P. C. Waterman, "Exact radar cross section of axisymmetric conducting targets," this issue, page 805.
[14] F. V. Schultz, G. M. Ruckgaber, S. Richter, and J. K. Schindler, "The theoretical and numerical determination of the radar cross section of a finite cone," School of Elec. Engrg., Purdue University, Lafayette, Ind., Rept. TR-EE64-14, Doc. AD 606 828, August 1964.
[15] A. Baghdasarian and D. J. Angelakos, "Solution of circular loop antennas and scattering from conducting loops by numerical methods," this issue, page 818.
[16] A. Sommerfeld, *Partial Differential Equations in Physics.* New York: Academic Press, 1949, pp. 29–31; 159–164.
[17] H. Margenau and G. M. Murphy, *The Mathematics of Physics and Chemistry.* New York: Van Nostrand, 1956, pp. 476–479.
[18] P. D. Crout, "A short method for evaluating determinants and solving systems of linear equations with real or complex coefficients," *AIEE Trans.* (*Supplement*), vol. 60, December 1941, pp. 1235–1241.
[19] R. G. Kouyoumjian, "The calculation of the echo areas of perfectly conducting objects by the variational method," Ph.D. dissertation, Dept. of Elec. Engrg., The Ohio State University, Columbus, December 1953.
[20] C. T. Tai, "Electromagnetic back-scattering from cylindrical wires," *J. Appl. Phys.*, vol. 23, pp. 909–916, August 1952.
[21] R. W. P. King and T. T. Wu, *The Scattering and Diffraction of Waves.* Cambridge, Mass.: Harvard University Press, 1959, pp. 153 and 161.
[22] Y. Y. Hu, "Back-scattering cross section of a center-loaded cylindrical antenna," *IRE Trans. on Antennas and Propagation*, vol AP-6, pp. 140–148, January 1958.
[23] J. H. Van Vleck, F. Bloch, and M. Hamermesh, "Theory of radar reflection from wires or thin metallic strips," *J. Appl. Phys.*, vol. 18, p. 274, 1947.
[24] R. W. P. King, *Theory of Linear Antennas.* Cambridge, Mass.: Harvard University Press, 1956, ch. 4.
[25] S. H. Dike and D. D. King, "Absorption gain and back-scattering cross section of the cylindrical antenna," *Proc. IRE*, vol. 41, pp. 926–934, July 1953.
[26] K. Lindroth, "Reflection of electromagnetic waves from thin metal strips," *Trans. Roy. Inst. Technol.* (*Stockholm*), no. 91, 1955.
[27] E. Hallén, "Exact solution of the antenna equation," *Trans. Roy. Inst. Technol.* (*Stockholm*), no. 183, 1961.